Collective model distorted-wave Born approximation analysis of 500-MeV proton scattering from ^{40}Ca

J. Lisantti,* D. J. Horen, F. E. Bertrand, R. L. Auble, B. L. Burks, E. E. Gross, and R. O. Sayer
Oak Ridge National Laboratory, Oak Ridge, Tennessee 37831

D. K. McDaniels
University of Oregon, Eugene, Oregon 97403

K. W. Jones, J. B. McClelland, and S. J. Seestrom-Morris
Los Alamos National Laboratory, Los Alamos, New Mexico 87545

L. W. Swenson
Oregon State University, Corvallis, Oregon 97331
(Received 5 August 1988)

A vibrational collective model has been used to analyze 15 bound states in ^{40}Ca excited by inelastic scattering of 500 MeV polarized protons. It is shown that for those states which have surface peaked charge transition densities the collective model describes the shape and magnitude of the angular distributions quite well. The hadronic deformation lengths extracted are shown to be constant over the incident proton energy range of 25–800 MeV with the exception of data at 185 MeV. The average values for the hadronic deformation lengths are used to calculate the ratio of the neutron to proton multipole matrix elements for five states. Elastic scattering and the 3_1^-, 2_1^+, and 5_1^- transitions have also been studied using the relativistic collective model.

I. INTRODUCTION

An increasing amount of evidence[1–3] is accumulating showing that the collective, deformed potential, model provides a valid description for low- and intermediate-energy inelastic proton scattering to collective states and giant resonances. The impetus for these studies came from several earlier investigations which seemed to imply a breakdown at intermediate energies of this model. The first results showing this anomalous behavior were obtained from measurements[4] of the excitation of the ISGQR (isoscalar giant quadrupole resonance) by 155-MeV protons, for a number of targets spanning the Periodic Table. The degree to which these transitions depleted the EWSR (energy weighted sum rule)[5] were deduced and found to be 30 to 50 %, compared to values of 60 to 80 % deduced at other energies.[5] Similar anomalous results for the measured ISGQR sum rule were obtained in several later experiments[6–8] with intermediate-energy protons.

In two of these experiments,[7,8] anomalous results were also obtained for some of the low-lying states in ^{208}Pb, particularly the 3^- state at 2.614 MeV. To explain these anomalous results, Osterfeld *et al.*[9] compared microscopic and macroscopic calculations for the first 3^- state in ^{208}Pb at several different incident proton energies up to 155 MeV. They interpreted the apparent lowering of the macroscopic prediction at 155 MeV with respect to the microscopic one as indicating that macroscopic model calculations were not reliable at this energy.

As noted above, more recent inelastic proton scattering studies have shown that the collective model was not at fault. In the case of the ISGQR measurements, the earlier anomalous results were due to a combination of experimental problems, including absolute normalization determinations,[7] a poor choice of optical-model parameters and difficulties with background subtraction.[10,11] Our study[1] of the excitation of the 3^- (2.614 MeV) state in ^{208}Pb showed that the hadronic deformation length, δ_H, extracted from the collective model analysis is constant up to 400 MeV at the $\pm 5\%$ level, and may in fact even be constant up to 800 MeV. In a more complete report[3] on the low-lying collective states of ^{208}Pb we have shown that δ_H is constant within uncertainties for incident proton energies between 35 and 800 MeV for the 3^- (2.614 MeV), 5_1^- (3.198 MeV), 5_2^- (3.709 MeV), 2^+ (4.086 MeV), and the 4^+ (4.324 MeV) levels. A recent reanalysis[12] of low-energy (few MeV) neutron inelastic excitation of the 3^- (2.614 MeV) state of ^{208}Pb yields a value of δ_H similar to what we deduce from proton scattering works.

Recently, Hintz *et al.*[13] proposed that deformation lengths deduced from collective model analyses (and the implied neutron-proton multipole moment ratios M_n/M_p) are energy dependent. These authors conclude that the extracted (M_n/M_p) values continuously decrease downward from 500 MeV to below 100 MeV. They also state the the values at the lower energies (25–65 MeV) tend to be close to the higher values obtained at 800 MeV. Hintz *et al.*[13] conclude that the observed energy

dependence is due to a deficiency in the high momentum parts of the central spin-independent (and/or spin-orbit) interactions used to generate the inelastic transition potentials. A similar statement about a possible energy dependence of δ_H extracted for the 3^- (3.74 MeV) state of ^{40}Ca has been noted by Frekers *et al.*[14] They suggest that in the region of maximum nuclear transparency around 200 MeV, the curve of $\delta_H(3^-)$ vs energy seems to exhibit a shallow minimum. Also, a low value for the deformation length of the 3^-, 3.74 MeV state in ^{40}Ca was obtained by a recent analysis[15] using both nonrelativistic and relativistic phenomenological potentials to analyze 181- and 800-MeV proton scattering.

In this paper elastic and inelastic scattering of 500-MeV polarized protons from ^{40}Ca are studied using both nonrelativistic and relativistic DWBA formalisms. Careful attention has been given to possible ambiguities in the optical-model potential parameters determined from fitting elastic scattering data in the nonrelativistic model. Using optical-model parameters determined from fits to the data, an analysis of inelastic scattering to 15 bound states in ^{40}Ca was made using a vibrational collective model. A comparison of theoretical and measured differential cross sections for the well-known low-lying collective states is used to test the validity of this model. We also compare our results to those of Seth *et al.*[16] who studied the collective model fits to five states (3_1^-, 3.74 MeV; 2_1^+, 3.90 MeV; 5_1^-, 4.49 MeV; 3_2^-, 6.29 MeV; 2_4^+, 6.91 MeV) in ^{40}Ca using 500-MeV protons. An interesting result of the analysis in Ref. 16 was that some states which have the same spin and parity (J^π) display quite different angular distributions. This was seen in a comparison of the 3_1^- and 3_2^-, 3_3^- states, as well as for the 2_1^+ and 2_4^+ states. Here we extend this study to other states in ^{40}Ca. We have also examined the contention of both Refs. 13 and 14 that the hadronic deformation length for the 3_1^- state is not independent of energy but exhibits a minimum in the 150–200-MeV region of incident proton energy. As a final theoretical analysis of the data we have analyzed elastic scattering and inelastic scattering to the 3_1^-, 2_1^+, and 5_1^- states using the relativistic collective DWBA formalism in a manner similar to that of Refs. 15 and 17.

For those states where the collective analysis is appropriate, and for which electromagnetic deformation lengths are known, the ratio of the neutron to proton multipole matrix elements (M_n/M_p) were deduced and compared with values obtained in other studies.

II. EXPERIMENTAL

The data described here were obtained as part of an experiment performed at the Clinton P. Anderson Meson Physics Facility (LAMPF) to study giant resonance excitations. The 500 MeV protons, polarized in a direction normal to the scattering plane, were scattered from a 49.88-mg/cm^2 ^{40}Ca target and were detected in the high-resolution spectrometer (HRS). The experimental resolution was approximately 70 keV (FWHM). A typical spectrum at a spectrometer angle of 16.5° is shown in Fig. 1. We have analyzed all of the peaks labeled on Fig. 1 including a state at 8.75 MeV which does not appear in the 16.5° data. For the known 2^+, 4^+ doublet at 5.249 and 5.279 MeV, respectively, we have assumed a single peak at 5.26 MeV, and its analysis will be discussed later. The unlabeled peaks seen in Fig. 1 arise from the excitation of more than a single state and consequently were not analyzed. In Fig. 2, data are shown for the region of 9–14 MeV of excitation energy. The level density is quite large and even with 70 keV resolution it is difficult to resolve peaks from the excitation of single ^{40}Ca levels. As in Fig. 1, we have analyzed only the peaks labeled in Fig. 2.

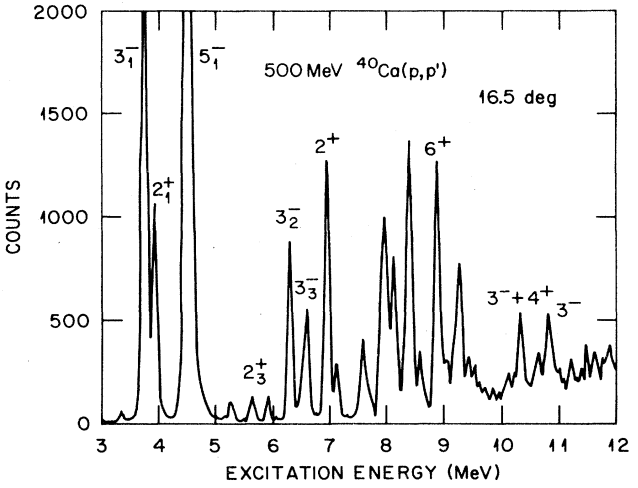

FIG. 1. Spectrum of ^{40}Ca(p,p')^{40}Ca* taken at a spectrometer angle of 16.5°.

The beam polarization for both spin-up and spin-down was measured periodically by placing a thin CH_2 target in an in-beam polarimeter located upstream from the HRS scattering chamber. The beam polarization was also continuously measured using the quench-ratio

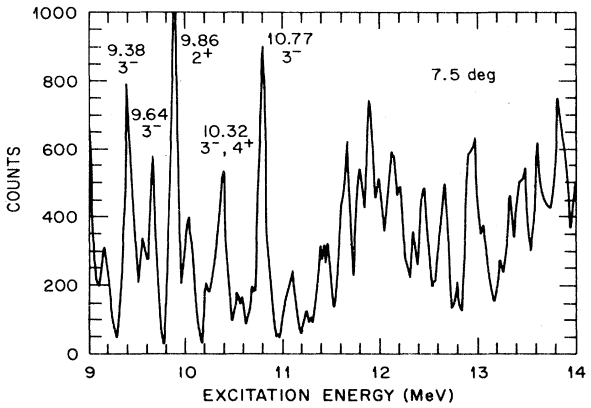

FIG. 2. Spectrum of ^{40}Ca(p,p')^{40}Ca* taken at a spectrometer angle of 7.5°.

method. In all cases the two methods agreed within a few percent. The beam polarization slowly varied between |0.80| and |0.87| during the course of the experiment. The beam current was measured with two in-beam ionization chambers located in the HRS scattering chamber downstream from the target position.

We normalized our elastic p-^{40}Ca scattering data to those from TRIUMF at 500 MeV.[18] A comparison of our inelastic cross sections for the 3_1^-, 3.736 MeV state, 2_1^+, 3.904 MeV state, and the 5_1^-, 4.49 MeV state was then made to another 500 MeV experiment done at LAMPF.[16] Our inelastic data were found to agree ($\pm 5\%$) with the inelastic data reported in Ref. 16.

Cross sections and analyzing powers were measured at laboratory angles of 4°, 7°, 10°, 12°, 14°, 17°, and 20°, and were binned into 0.5° increments in the off-line analysis. The angle resolution of the spectrometer is approximately 0.1°. Since this experiment was primarily concerned with measurements of the giant resonance region, good statistics were accumulated for the bound states, as can be seen in Fig. 1.

III. RESULTS AND NONRELATIVISTIC COLLECTIVE MODEL CALCULATIONS

We present in this section the results of calculations performed in nonrelativistic DWBA and using the standard collective, deformed potential, vibrational model. Fifteen bound states in ^{40}Ca were studied. The optical potential is given as

$$U = V_C - V_R f_R - V_I f_I + \left[\frac{\hbar}{m_\pi c}\right]^2 \frac{1}{r}\frac{d}{dr} \times (V_{\mathrm{RSO}} f_{\mathrm{RSO}} + V_{\mathrm{ISO}} f_{\mathrm{ISO}}) \sigma \cdot l \ , \quad (1)$$

with V_C as the Coulomb, V_R real, V_I imaginary, V_{RSO} real spin-orbit, and V_{ISO} imaginary spin-orbit potential depths.

The potential shape comes from the function f_x which has the usual Woods-Saxon form

$$f_x = \frac{1}{1+e^{(r-r_x A^{1/3})/a_x}} \ , \quad (2)$$

with the parameters r_x and a_x being the radius and diffuseness associated with each part of the optical potential. Thus, there are 12 independent parameters which have to be determined from fits to elastic scattering data. This results in a certain amount of ambiguity, and this was studied in some detail.

In the vibrational model, the transition potential is obtained by taking the radial derivative of the optical potential with the strength proportional to the deformation length, δ_H, so its radial parts have the form

$$G_i(r) = -\delta_{Hi}\frac{dU_i}{dr} \ , \quad (3)$$

where U_i refers to each of the components in Eq. (1) except for V_C. This transition potential is then used to calculate the inelastic cross sections and analyzing powers for the low-lying collective states. The only adjustable parameter in the inelastic calculations is the hadronic deformation length, δ_H. In general, each of the five terms of the transition potential may have a different deformation length associated with it. However, it is frequently assumed that all the deformation lengths are equal, although in some cases better fits to analyzing power data have been obtained when the deformation lengths of the spin-orbit terms are adjusted to be in the range of 0.75 to 1.5 times those of the central potentials.[19] All of the calculations discussed here were done with the program ECIS79 (Ref. 20) and with the five deformations lengths set equal.

In order to obtain the 12 optical-model parameters we performed a search on cross section and analyzing power data for elastic p-^{40}Ca scattering at 300, 400, and 500 MeV.[18] The results are presented in Table I with the fits to the data shown in Figs. 3–5. The best fit at 500 MeV gave a large value for the real radius which was judged to be unphysical. Hence, at this energy the real radius and diffuseness were fixed at the average of the values obtained at 300 and 400 MeV. We then searched on the remaining 10 parameters for the 500 MeV data. These results are shown in the last column of Table I, and will be referred to as set I. Set I contains the optical-model parameters which are then used for calculating inelastic scattering. Table II contains optical-model parameters determined from other analyses of 500 MeV p-^{40}Ca elastic scattering, set II is from Ref. 16, while set III is from Ref. 21. The parameter set II was obtained by fitting elastic scattering data which extended over an angular re-

TABLE I. Optical-model parameters for 300, 400, and 500 MeV ^{40}Ca(p,p) elastic scattering. The column on the farthest right results from an average geometry of the real potential for 300 and 400 MeV and is set I. Potential depths in MeV, length in fm.

	300 MeV	400 MeV	500 MeV	500 MeV (Set I)
V_R	4.11	4.79	0.32	0.51
r_R	1.385	1.369	1.642	1.377
a_R	0.690	0.740	0.407	0.715
V_I	21.81	21.87	59.94	50.50
r_I	1.150	1.193	0.971	1.022
a_I	0.690	0.601	0.650	0.620
V_{RSO}	2.61	1.69	1.34	1.281
V_{RSO}	1.025	1.058	1.136	1.135
a_{RSO}	0.629	0.652	0.628	0.657
V_{ISO}	−2.98	−2.98	−3.50	−3.22
r_{ISO}	0.998	1.045	0.876	0.934
a_{ISO}	0.676	0.620	0.833	0.760
r_c	1.2	1.2	1.2	1.2
$\frac{\chi^2}{N}\sigma$	8.76	11.05	7.36	8.97
$\frac{\chi^2}{N}A_Y$	6.04	9.87	8.45	5.55

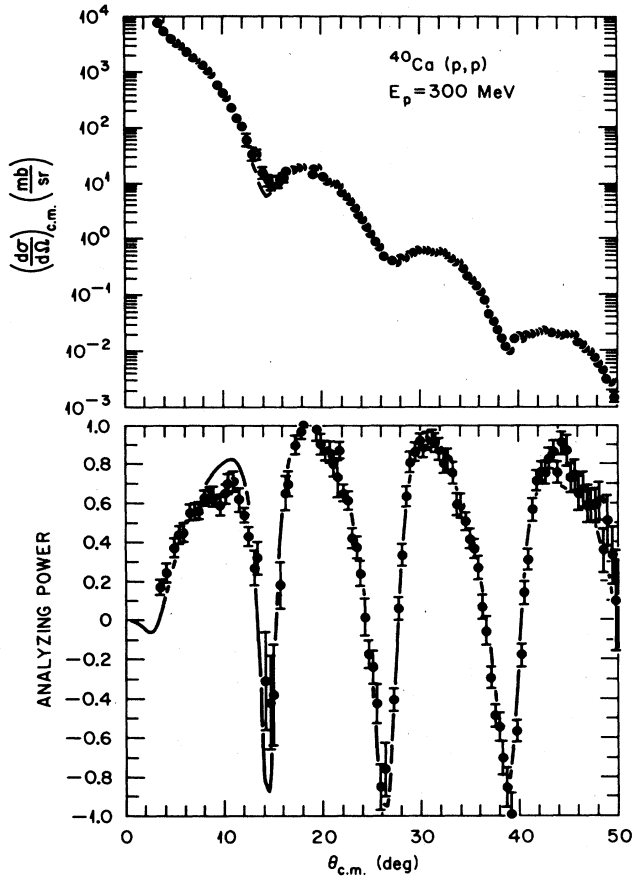

FIG. 3. Fits to 300 MeV ^{40}Ca(p,p') elastic scattering. Optical-model parameters used are in Table I.

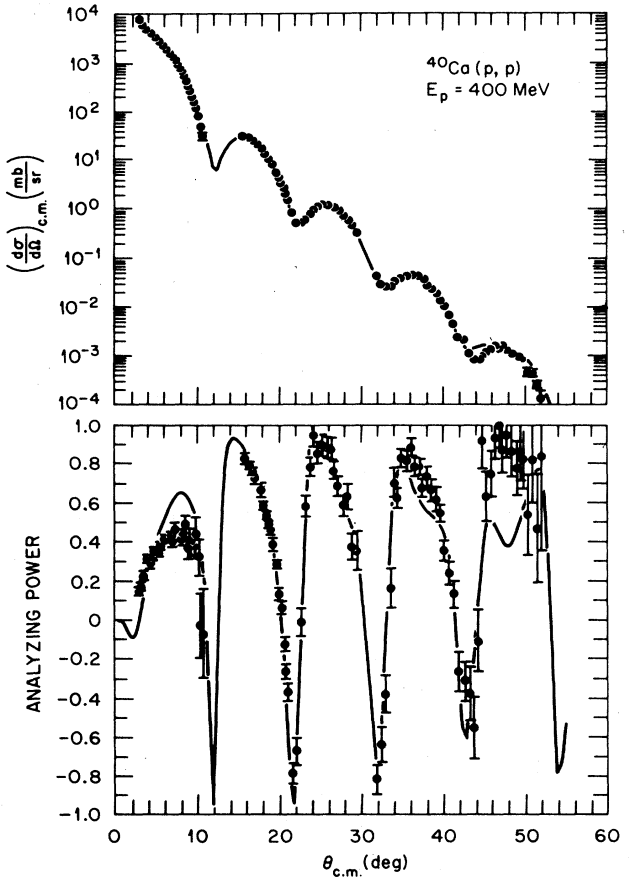

FIG. 4. Fits to 400 MeV ^{40}Ca(p,p') elastic scattering. Optical-model parameters used are in Table I.

gion of approximately 5°–29° in the center of mass, while the parameters in set III are from fits to the same data as used in the present work. In both cases the real potential is repulsive, whereas our results yield a weakly attractive one. In Fig. 5 we show fits to the 500 MeV elastic data of Ref. 18 using the optical parameters determined from the present work as well as those of sets II and III. For the cross section data at angles forward of about 30°, sets I and II describe the data about equally well, while set III gives a poorer fit. At the angles larger than 30° none of these parameter sets fit the data. The analyzing power data forward of 30° are best fit using sets I or II, while the larger angle data are best fit with sets I and III. While sets II and III are much closer to one another in their numerical values it is interesting to see the large differences in their calculated elastic cross sections and analyzing powers. The largest differences in all three optical-model sets are in the parameters for the real potential. Yet the fits to the elastic scattering data do not show a strong preference for any of the three sets of optical-model parameters. This may imply that the calculated cross section and analyzing powers at this energy are not sensitive to the shape of the real potential. In a recent work[22] which studied 500 MeV proton scattering from ^{40}Ca, optical potentials were generated in a microscopic $t\rho$ formalism (i.e., the convolution of the interaction t with the ground state density ρ), in both a nonrelativistic and relativistic framework. The potentials for the imaginary central, and real and imaginary spin-orbit terms were similar in each model and similar to the phenomenological collective potentials used in the present work. However, the real potential shapes were drastically different from one another and from the present work. While it is difficult to directly compare the effect of two different potential shapes using two different reaction models, it has been shown in Ref. 22 that there were no significant differences in the deformation lengths deduced from inelastic cross sections in a comparison between the two reactive models and in a comparison to phenomenological results (present paper). Since elastic and inelastic calculations using set II have been published[16] we will not use them in any of our other calculations, and instead we will use sets I and III.

Figure 6 shows our cross section and analyzing power data for the 3_1^-, 3.736 MeV, 2_1^+, 3.904 MeV, and the 5_1^-, 4.49 MeV states compared with results of calculations using the optical model parameter sets I and III. The cross sections for all three states are reproduced fairly well

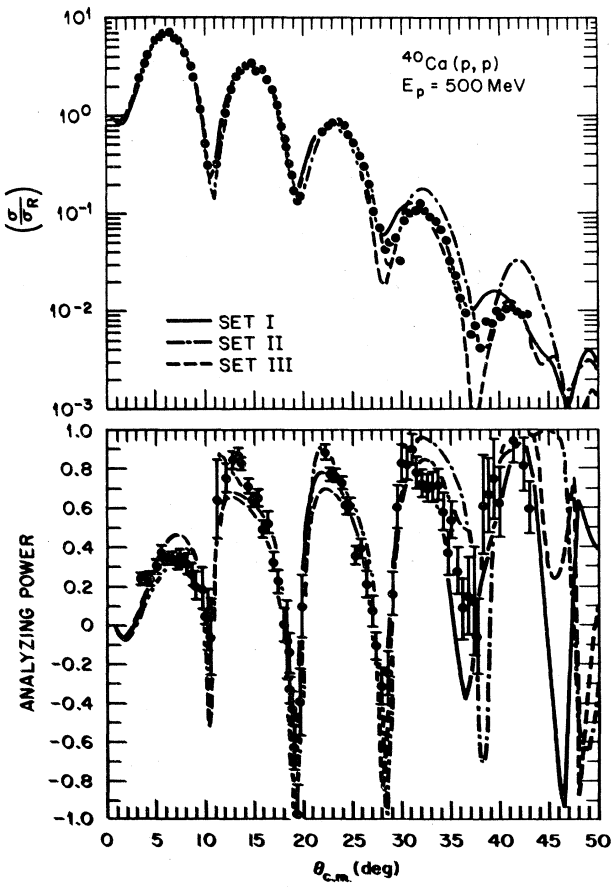

FIG. 5. Elastic scattering angular distributions from the data of Ref. 18 with fits using the optical-model parameters in Tables I and II.

TABLE II. Optical-model parameters for 500 MeV ^{40}Ca(p,p) elastic scattering, potential depths are in MeV, lengths are in fm.

	Set II[a]	Set III[b]
V_R	−28.3	−28.17
r_R	0.79	0.70
a_R	0.44	0.79
V_I	41.4	36.63
r_I	1.08	1.04
a_I	0.650	0.79
$V_{\rm RSO}$	2.87	3.35
$r_{\rm RSO}$	0.91	0.99
$a_{\rm RSO}$	0.68	0.75
$V_{\rm ISO}$	−2.90	−2.80
$r_{\rm ISO}$	1.04	1.08
$a_{\rm ISO}$	0.60	0.68
r_c	1.2	1.2
$\frac{\chi^2}{N}\sigma$	108.6	12.8
$\frac{\chi^2}{N}A_Y$	14.0	9.1

[a]Reference 16, spin-orbit potentials divided by 4 to take into account the absence of the pion Compton wavelength $(\hbar/m_\pi c)^2 \approx 2$, and spin factor of 2 which arises because of $L\cdot S$ compared to $L\cdot\sigma$ which ECIS79 uses.
[b]Reference 21, potential depths divided by relativistic factor $\gamma = 1.48$.

with both sets.

The analyzing power data shown in Fig. 6 are also fit fairly well using either of the optical-model parameter sets with the 2_1^+ state favoring set III, and the 5_1^- state favoring set I. The parameters of set II provide good fits (as shown in Ref. 16) for the 2_1^+ state, but fail to fit the 3_1^- and 5_1^- states at forward angles. While parameter sets I and III both lead to reasonable fits overall to the data of Figs. 5 and 6, we have used parameter set I for the remainder of the analysis because it was determined from a search of the 300, 400, and 500 MeV data. However, reference will be made below to the deformation length values obtained with parameter set III for comparison. Values of δ_H (in fm) from set I and set III are also shown in Fig. 6.

Plotted on Fig. 7 are the experimental cross sections for the other states shown in Figs. 1 and 2 compared with collective model DWBA calculations which best describe these states. Only the 2_3^+ (5.63) MeV state, 2^+ (8.75 MeV) state, 6^+ (8.85 MeV) state, 3^- (9.38 MeV) state, and the 2^+ (9.86 MeV) state are adequately described in shape by the model. In a similar study using 800 MeV protons Adams *et al.*[23] obtained similar fits for the 2_3^+, 5.63 MeV and the 6^+, 8.85 MeV states. These authors do not report data for the 2^+, 8.75 MeV state or for any of the states above and including the 3^- at 9.38 MeV. They also note the failure to the fit the data for the 3^- states at 6.29 and 6.58 MeV with collective model transition potentials of the form given in Eq. (3). We were unable to fit the 2^+, 4^+ doublet at 5.26 MeV with either multipolarity or a combination of the two. We have shown an $L=2$ transfer for this state just for reference. The authors of Ref. 23 also tried to fit data for the 5.26 MeV 2^+ (5.249 MeV), 4^+ (5.279 MeV) doublet, but they were unable to do so adequately. This may imply that either or both of these states do not have surface peaked transition potentials. For the state at 6.93 MeV, the multipolarity that gave the closest fit to the data was $L=2$. A state at 6.918 MeV was reported in Ref. 23 and a similar fit was obtained with $L=2$. The work of Ref. 16, while not showing fits to the 3_2^-, 6.29 MeV, and 2^+, 6.91 MeV states, does find that the angular distributions for these states are quite different from those for the 3_1^- and 2_1^+, respectively. A state at 10.32 MeV was found but could not be fitted with a single multipolarity. We assign it as a 3^-, 4^+ doublet with the data at small angles having a possible contribution from the 1^+, $T=1$ state at 10.32 MeV. A state at 10.77 MeV was also observed, and the closest fit was obtained by assuming it to be 3^-; however the resolution of the present experiment (70 keV) may not be adequate to resolve the levels in this region. It would

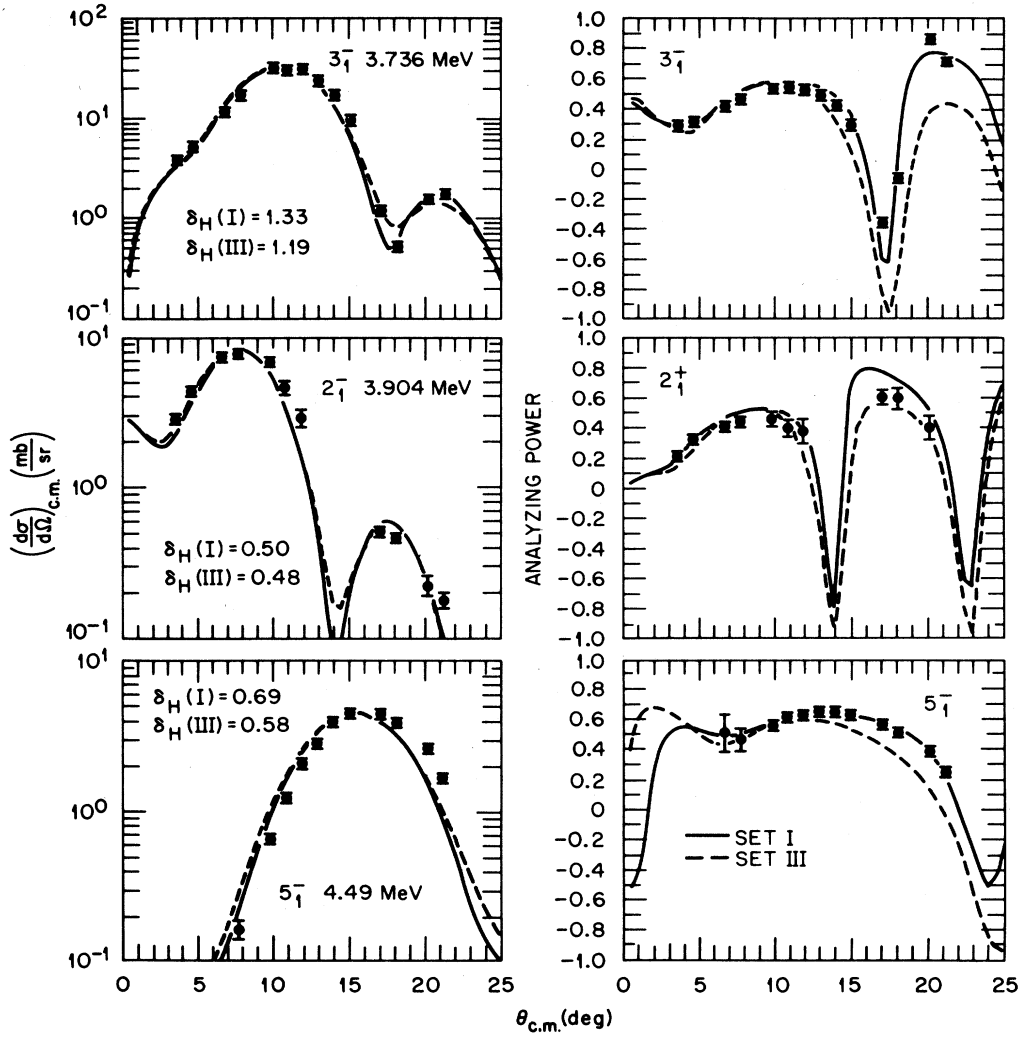

FIG. 6. Angular distributions for the 3_1^- (3.736 MeV), 2_1^+ (3.904 MeV), and the 5_1^- (4.49 MeV) states. The δ_H is the deformation length (in fm) of the optical potential. The calculated cross sections were obtained using ECIS79.

appear that the states at 6.29, 6.58, and 6.93 MeV cannot be adequately described by using the simple collective model form factor. A possible reason for this will be discussed later in this paper.

IV. RELATIVISTIC COLLECTIVE MODEL CALCULATIONS

In this section we present an analysis of elastic scattering and inelastic scattering to the 3_1^-, 2_1^+, and 5_1^- states using the formalism of the phenomenological Dirac collective model.[15] In this model the optical potential as used in the Dirac equation is given as

$$U_{\text{opt}} = U_s(r) + \gamma^0[U_v(r) + U_C(r)] , \quad (4)$$

where $U_s(r)$ is the scalar potential, $U_v(r)$ is the vector potential, $U_C(r)$ is the Coulomb potential, and γ^0 is the Dirac matrix. The scalar and vector potentials have both real and imaginary components, and are assumed to have a Woods-Saxon shape. Therefore, as in the phenomenological nonrelativistic collective calculations presented in Sec. III, the relativistic model also has 12 free parameters which are found from fitting elastic scattering data. Well-known ambiguities exist in searching for optical-model parameters to use in the Dirac formalism, especially in the imaginary parts of the potential.[17,24] A recent application[17] of the phenomenological Dirac model to 500-MeV proton elastic scattering from ^{40}Ca has studied these ambiguities and has arrived at various sets of optical-model parameters in which the imaginary vector potential (W_v) has been varied between 0 and -180 MeV. The best fits[17] to cross section and analyzing power data were obtained with the parameter sets having W_v ranging from -80 to -120 MeV. We have performed an analysis of the data from Ref. 18 using the program ECIS87.[20] The data of Ref. 18 extend to larger scattering angles than the data[16] used in the search re-

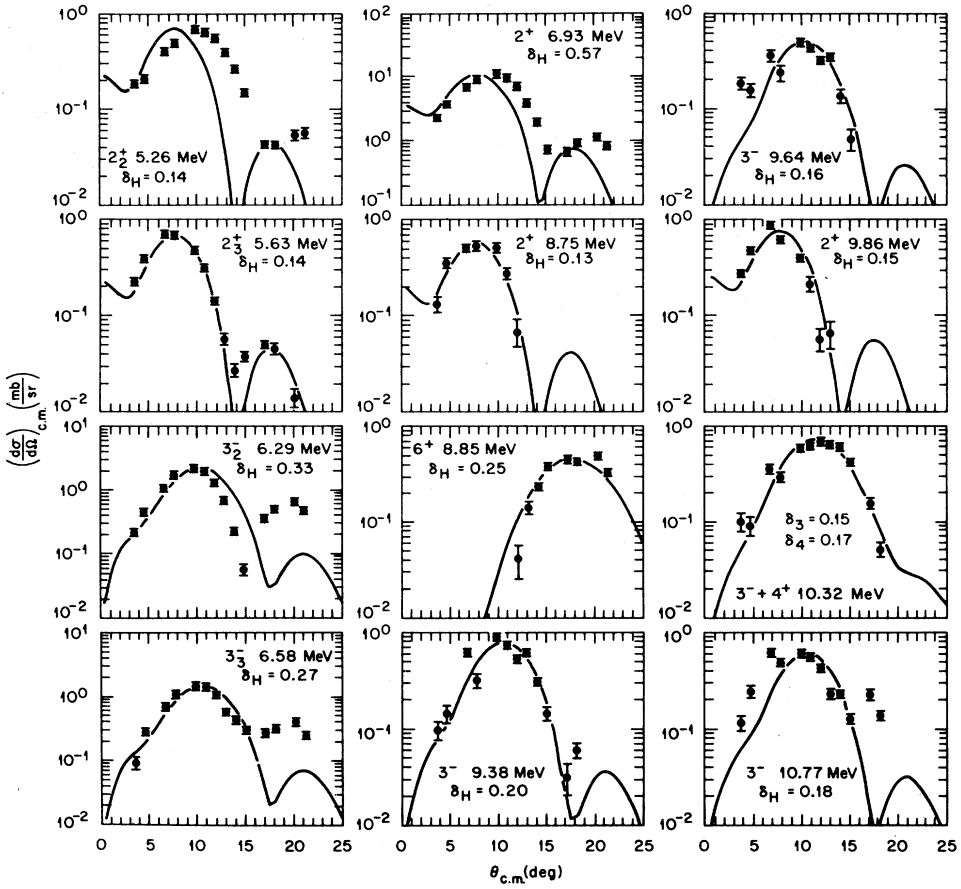

FIG. 7. Angular distributions for remaining fitted states. The calculations shown are from ECIS79.

ported in Ref. 17 (43° in σ and A_y vs 29° in σ and 35° in A_y). We find that our analysis of the elastic scattering data is unable to choose between an imaginary vector potential value of -80 to -120 MeV as is shown in Fig. 8. As can be seen in this figure, the fits to the cross-section data are of similar quality to that using the nonrelativistic models. The fit to the analyzing power data is superior to the fits obtained using the nonrelativistic model. However, the author of Ref. 17 has shown that the spin rotational parameter Q favor $W_v = -80$ MeV over $W_v = -140$ MeV (no result for $W_v = -120$ MeV was shown).

Using the optical-model parameters of Ref. 17 with $W_v = -80$ and -120 MeV, we calculated the cross sections and analyzing powers for the 3_1^-, 2_1^+, and 5_1^- states using the relativistic collective model.[15,17] Unlike Ref. 17 we have used the same deformation length, constant for each of the four terms of the transition potential; Coulomb excitation was not included. The results of these calculations are compared with the present data in Fig. 9. The fits to the differential cross sections are quite similar to those obtained using the nonrelativistic model. A more comprehensive discussion of the deformation lengths obtained in our analysis will be presented in Sec. VI. The analyzing power data for the 3_1^- and 2_1^+ states are described slightly better using the relativistic model, while the nonrelativistic model fits the 5_1^- data better. The inelastic scattering data also show no sensitivity to the value of the imaginary vector potential (W_v), both -80 and -120 MeV giving equally good fits to the data.

V. MULTIPOLE MATRIX ELEMENTS

Potential deformation lengths extracted for eight states in ^{40}Ca are presented in Table III along with values obtained using protons of other energies. Figure 10 shows the deformation lengths for the 3_1^-, 2_1^+, and 5_1^- states plotted versus incident proton energy. The general trend of the data (except 185 MeV) suggest little (if any) energy dependence. Assuming that the observed deformation lengths are independent of energy, the weighted average (weighted by the experimental uncertainty) of the deformation lengths and associated uncertainties are tabulated in Table III (we have not used the values found at 155 and 185 MeV and the reason for omitting these are given in Sec. VI). We utilize the average values to estimate M_n/M_p ratios.[25]

The multipole matrix element for each transition is defined as

$$M_{n,p} = \int_0^\infty \rho_{\rm tr}^{n,p}(r) r^{\lambda+2} dr \ , \qquad (5)$$

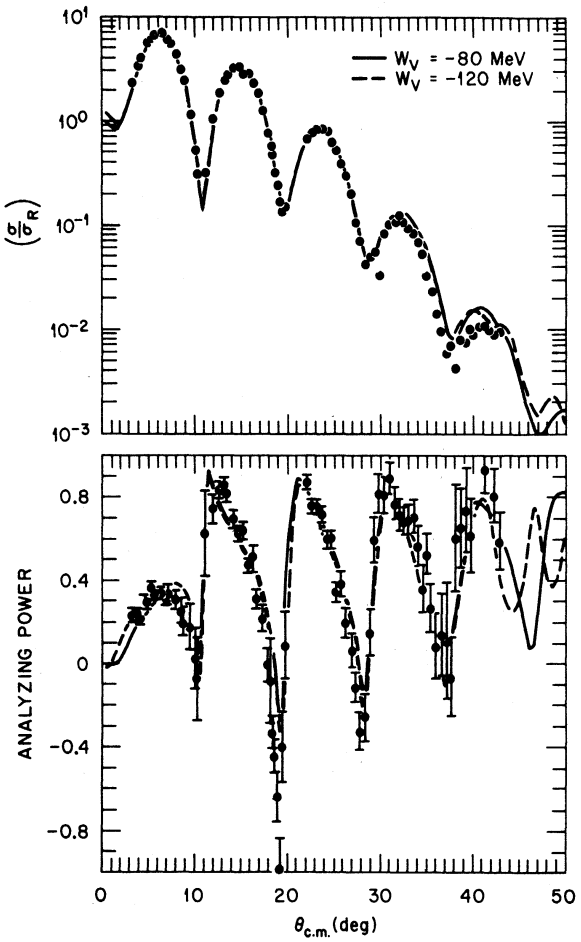

FIG. 8. Elastic scattering angular distributions from the data of Ref. 18. The curves are from the relativistic model using $W_V = -80$ and -120 MeV parameters of Ref. 17 in ECIS87.

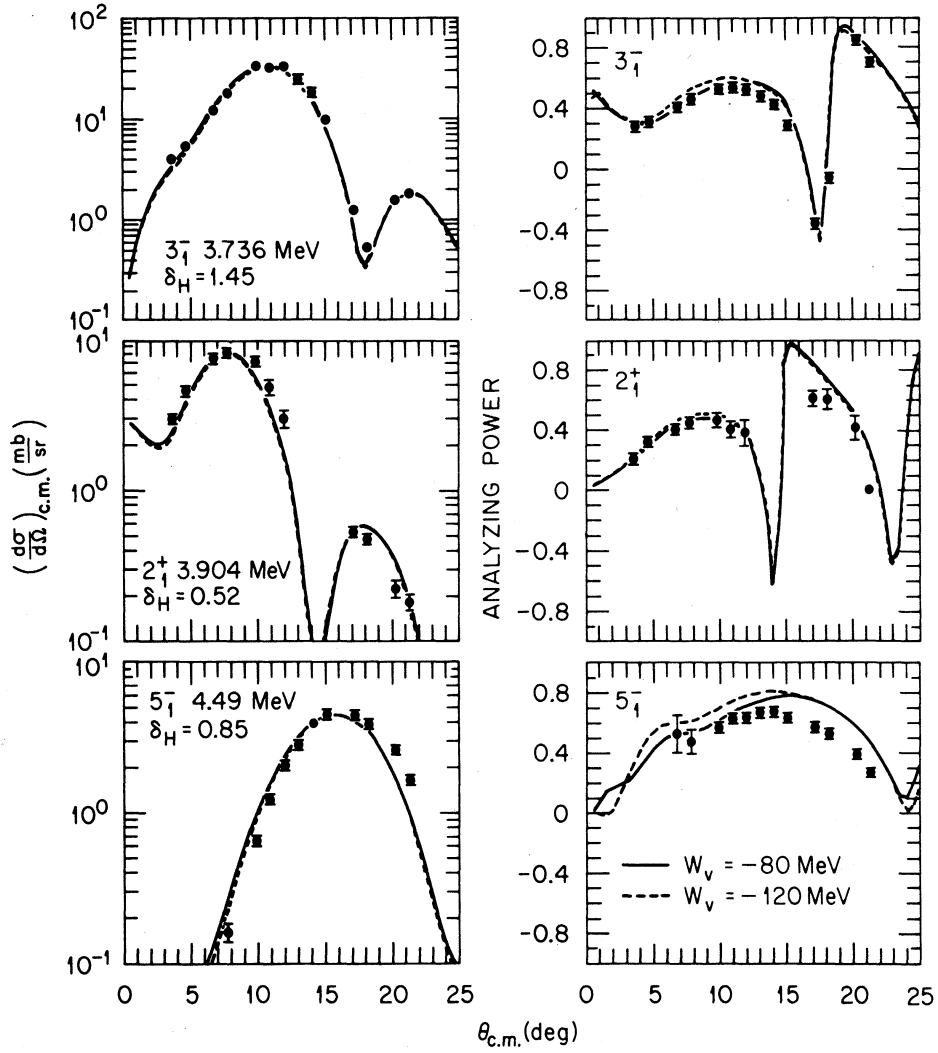

FIG. 9. Angular distributions for the 3_1^- (3.736 MeV), 2_1^+ (3.904 MeV), and the 5^- (4.49 MeV) states. The calculations shown are from the relativistic model using ECIS87.

TABLE III. Potential deformation lengths as determined with the nonrelativistic model for states in ^{40}Ca excited by (p,p'), units are in fm.

E_p (MeV)	3_1^- 3.736	2_1^+ 3.904	5_1^- 4.49	2^+ 5.63	2^+ 8.75	6^+ 8.85	3^- 9.38	2^+ 9.86
25[a]	1.40±0.03	0.42±0.01	0.91±0.02		0.17±0.01			
30[a]	1.38±0.03	0.43±0.01	0.86±0.02		0.15±0.01			
35[a]	1.35±0.03	0.42±0.01	0.83±0.02		0.15±0.01		0.16±0.01	
40[a]	1.32±0.03	0.43±0.01	0.80±0.02		0.14±0.01			
185[b]	1.05±0.10	0.49±0.05	0.57±0.06					
334[c]		0.43±0.04		0.13±0.02	0.12±0.02			0.14±0.02
362[d]	1.22	0.42	0.69					
500[e]	1.33±0.03	0.50±0.03	0.69±0.03	0.14±0.01	0.13±0.02	0.25±0.01	0.20±0.03	0.15±0.03
500[f]	1.41±0.04	0.49±0.01	0.86±0.03					
800[g]	1.39±0.08	0.52±0.03	0.76±0.05	0.15±0.01		0.28±0.02		
δ_H[h]	1.35	0.44	0.83	0.14	0.15	0.26	0.17	0.14
σ[i]	0.01	0.01	0.01	0.01	0.01	0.01	0.01	0.02
δ_p	1.40±0.05[j]	0.48±0.05[j]	0.74±0.05[j]	0.13±0.03[k]	0.13±0.01[k]			

[a]C. R. Gruhn *et al.*, Phys. Rev. C **6**, 915 (1972).
[b]Analysis of elastic data from Ref. 31, and using inelastic data from Ref. 29, provided by H. Sherif.
[c]D. J. Horen *et al.*, Phys. Rev. C **30**, 709 (1984).
[d]Reference 14, no uncertainty given.
[e]Present work.
[f]Reference 16.
[g]Reference 23.
[h]Weighted mean, data from 25 to 500 MeV ignoring 155 and 181 values (see text).
[i]Weighted standard deviation.
[j]Reference 26.
[k]R. Moreh *et al.*, Phys. Rev. C **25**, 1824 (1982).

with λ being the angular momentum and $\rho^i_{\rm tr}(r)$, $i=n$ or p being the transition density. It is assumed that the transition density $\rho^i_{\rm tr}(r)$ for collective excitations is given by the derivative of the ground-state density in the same way that the transition potential [Eq. (3)] is assumed to be given by the radial derivative of the optical potential; i.e., we assume that

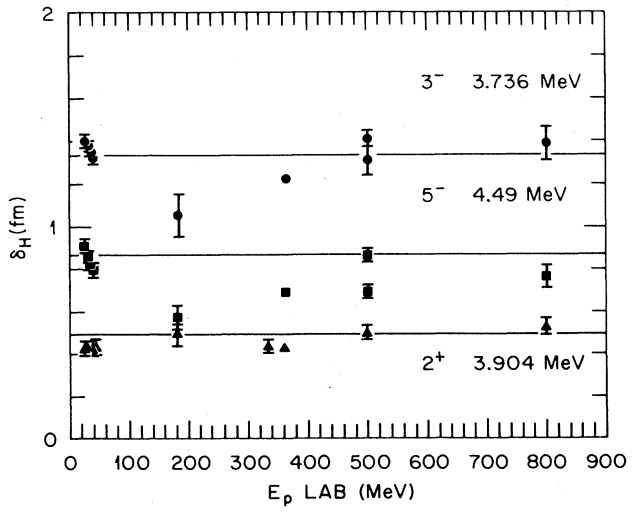

FIG. 10. Deformation lengths for the 3_1^- (3.736 MeV, circles), 2_1^+ (3.904 MeV, triangles), and 5_1^- (4.49 MeV, squares) states at various incident proton energies.

$$\rho^i_{\rm tr}(r) = -\delta_i \frac{\partial \rho i}{\partial r} \ . \tag{6}$$

If ρ_n, ρ_p (the ground-state n,p density distributions) have the same radial shape then

$$\frac{M_n}{M_p} = \left[\frac{N}{Z}\right]\left[\frac{\delta_n}{\delta_p}\right] . \tag{7}$$

It has been shown[25] that the potential deformation length is related to the density deformation lengths in this model by

$$\delta_H = \frac{Z\delta_p + FN\delta_n}{Z + FN} \ , \tag{8}$$

where F is the ratio of the strength of the neutron-proton interaction to the proton-proton one. The proton deformation length, δ_p, is also given by the $B(E\lambda)\uparrow$ for the transition by

$$\delta_p = \left[\left[\frac{4\pi}{Z(\lambda+2)}\right]^2 B(E\lambda)\uparrow \frac{1}{\langle r^{\lambda-1}\rangle^2}\right]^{1/2} . \tag{9}$$

Using Eqs. (7) and (8), we get the ratio of the neutron-to-proton multipole matrix elements in terms of the measured potential deformation length, δ_H, and the proton deformation length, δ_p,

$$\frac{M_n}{M_p} = \frac{N}{Z}\left[\frac{\delta_H}{\delta_p} + \frac{Z}{FN}\left[\frac{\delta_H}{\delta_p} - 1\right]\right] . \tag{10}$$

TABLE IV. Ratio of neutron to proton multipole matrix elements M_n/M_p.

State		25–500 MeV (p,p')	800 MeV (p,p')[a]	500 MeV (p,p')[b]
3^-	3.736 MeV	0.93±0.07	0.99±0.08	0.90
2^+	3.904 MeV	0.84±0.20	1.2 ±0.2	0.98
5^-	4.49 MeV	1.24±0.15	1.06±0.15	
2^+	5.63 MeV	1.15±0.52		
2^+	8.75 MeV	1.28±0.23		

[a]Reference 26.
[b]Reference 27, no uncertainty given.

Using the values of δ_H (from 25 to 500 MeV) and δ_p from Ref. 26 the calculated M_n/M_p ratios are tabulated in Table IV. The results given in Table IV suggest that $\delta_H \approx \delta_p$ for five states in ^{40}Ca. Also shown are the values determined at 800 MeV,[26] and recent results[27] of a reanalysis of earlier 500 MeV data,[16] obtained using a phenomenological effective interaction for the calculations.

In general, agreement between the determinations is considered good. The values of M_n/M_p listed in Table IV agree closely within the experimental uncertainties with the collective model result of 1.0 (i.e., $N/Z=1$), and this implies that these five states are predominantly isoscalar excitations.

VI. DISCUSSION

The present experiment provides high-resolution angular distributions for 15 bound states in ^{40}Ca excited by 500 MeV protons. The optical parameters used in the nonrelativistic analysis were obtained by fitting elastic scattering cross section and analyzing power data at 300, 400, and 500 MeV. Fits obtained with these parameters describe the elastic and inelastic data and were similar to fits obtained using other optical parameter sets[16,21] quoted in the literature.

Similar to our previous work on ^{208}Pb, we find that for ^{40}Ca also the hadronic deformation lengths for collective bound states are nearly independent of incident proton energies between 25 and 800 MeV. The earlier suggestion[9] that DWBA calculations using the macroscopic deformed potential collective model do not reproduce the data has not been substantiated by our results[1,3] for ^{208}Pb or from the present work for ^{40}Ca.

We find that the δ_H values for the 3_1^- (3.736 MeV) and other states in ^{40}Ca are independent of incident proton energy contrary to the results from Refs. 13 and 14. It is argued in those works that δ_H for the 3^- state in ^{40}Ca exhibits a minimum near 200 MeV, based on data obtained with incident proton energies of 155 MeV (Ref. 28) and 185 MeV.[29] The 155 MeV data of Ref. 28 had an experimental resolution of 600 keV which probably led to difficulty in separating the 3_1^- and 2_1^+ states at 3.736 and 3.904 MeV, respectively. Also, in a comparison to other data also obtained at 155 MeV,[30] the cross sections reported in Ref. 28 are approximately only 60% as large as those reported in Ref. 30. This may be related to the fact that the 3_1^-, and 2_1^+ states were resolved in Ref. 28 but not in Ref. 30. However, considering the resolution of both experiments and the disagreement in cross sections, it may be misleading to use either of those data sets. While the 185 MeV results were obtained with a resolution of 250 keV, they may also have had problems resolving the 3_1^- (3.736 MeV) state from the 2^+ (3.904 MeV) state. We have reanalyzed cross sections reported for 185 MeV using optical-model parameters from Ref. 21 which were obtained by fitting elastic scattering cross section and analyzing power measurements at 181 MeV.[31] We get a good fit to the elastic data, and achieve fits for the inelastic data of the same quality as those from our inelastic data at 500 MeV and as good as those shown in Ref. 15. However, as shown in Table III, the δ_H's for the 3_1^- and 5_1^- state are abnormally low compared to the rest of the results deduced at other energies, while the 2_1^+ state agrees with the other data. Given the observation that the hadronic deformation length as deduced from other proton inelastic scattering measurements has been shown to be constant from 25 to 500 MeV for five states in ^{208}Pb,[3] for two states in ^{28}Si (2^+, 1.78 MeV; 4^+, 4.62 MeV),[32] and three states in ^{12}C (2^+, 4.44 MeV, 3^-, 9.65 MeV, 4^+, 14.08 MeV),[2] we suggest that the cross section at 185 MeV are anomalously low, and therefore, we have not used them in our calculations of the average δ_H. We feel that it is important to measure angular distributions for elastic and low-lying collective states for ^{40}Ca and other nuclei in the 100-to-200 MeV incident proton energy range in order to resolve this question with ^{40}Ca. Based on the clear trend of the data shown in Table III we concur with the suggestion of Ref. 14 that the small values of the hadronic deformation lengths obtained at 155 and 185 MeV may be due either to inadequate optical-potential parameters, or to some experimental difficulties in calculating absolute cross sections.

An analysis of our data was also performed using the phenomenological Dirac formalism in a manner similar to that used in Refs. 15 and 17. The deformation lengths obtained for our data at 500 MeV along with results obtained by Ref. 15 at 181 and 800 MeV are presented in Table V. Our results at 500 MeV agree very well with the

TABLE V. Hadronic deformation lengths for states in ^{40}Ca obtained using the phenomenological Dirac formalism, units are in fm.

E_p (MeV)	3_1^- 3.736	2_1^+ 3.904	5_1^- 4.49
181[a]	1.014		
362[b]	1.22	0.42	0.69
500[c]	1.45±0.07	0.52±0.03	0.85±0.04
800[a]	1.289		
δ_H[d]	1.35±0.01	0.44±0.01	0.83±0.01

[a]Reference 15.
[b]Reference 14.
[c]Present work.
[d]Values obtained using phenomenological nonrelativistic formalism, see Table III.

nonrelativistic results presented on the bottom row of Table IV except for the 2_1^+ state for which the relativistic treatment yields a slightly higher value than the nonrelativistic formalism. Except for the 3_1^- value at 181 MeV, and taking into account the lack of uncertainties in their analysis, and deformation lengths obtained show no energy dependence in the Dirac formalism applied to these three states.

The collective model transition potential is surface peaked at the optical-model radius. If the microscopic transition charge density as determined by inelastic electron scattering has a shape and centroid similar to this surface peaked form, then it is expected that the macroscopic collective model calculation should describe the experimental angular distributions. Figure 11 shows the transition potential shapes from the collective model ($dU_{\rm opt}/dr$) (the major portion of the inelastic cross section at 500 MeV comes from the imaginary transition potential) compared with the transition densities deduced from inelastic electron scattering[33] for the 3_1^-, 3_2^-, and 3_3^- states. The shapes are similar for the 3_1^- state where the cross section at 500 MeV is fit quite well using the collective model. The 3_2^- and 3_3^- states have transition densities which are similar to each other but markedly different from that for the 3_1^- states. Likewise, their angular distributions are also similar to each other and differ from that of the 3_1^- state, and cannot be fit by DWBA calculations using the deformed potential model.

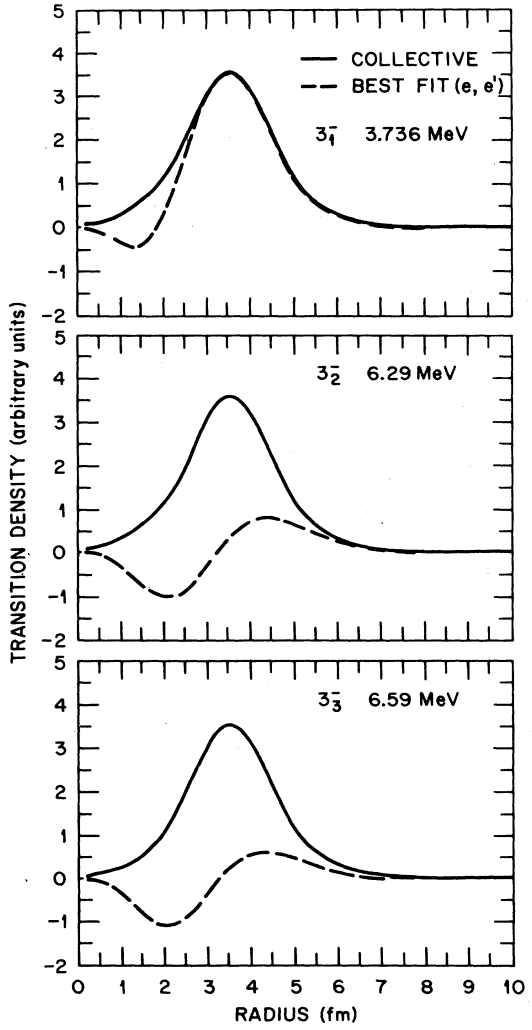

FIG. 11. Imaginary transition potentials obtained using the collective model compared to best-fit (Ref. 33) charge transition densities obtained from inelastic electron scattering.

In analogy with the results noted above, we suggest that the states at 5.63 MeV (2^+), 8.75 MeV (2^+), 8.85 MeV (6^+), 9.38 MeV (3^-), and 9.86 MeV (2^+) all have surface peaked charge transition densities, whereas the remaining states shown in Fig. 7 whose angular distributions are not well described by the deformed potential model have quite different transition densities.

Figure 12 shows the data for the 3_2^- (6.29 MeV) state compared with two calculations. The solid curve represents the predictions obtained using the collective model transition potential (the same as the calculation in Fig. 7). The dashed curve is the result of a calculation in which the shape of the form factor was taken as that of the transition charge density given in Ref. 33. Note that this transition potential shape fits the measured angular distribution (the calculation was normalized to match the data near 10°). This is interesting in that the assumed transition potential would result if the interaction between the proton and each target nucleon had a very short range, although it is believed that the effective nucleon-nucleon interaction at 500 MeV has a range of at least 1.4 fm.[34]

The results given in Table IV show that $\delta_H \approx \delta_p$ for five states in ^{40}Ca. When simple assumptions are used to re-

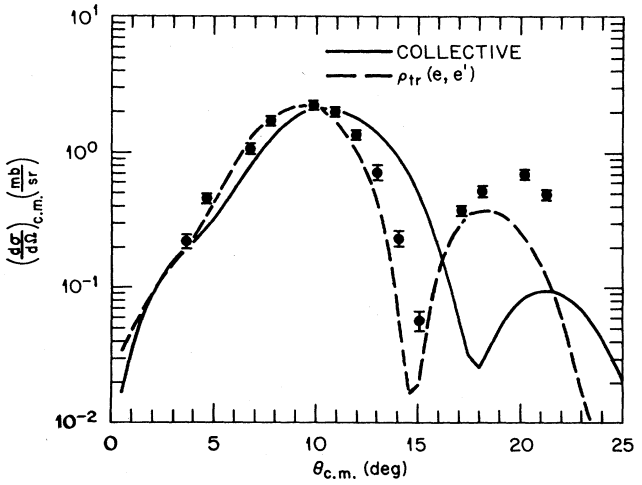

FIG. 12. Cross section data for the 3_2^- (6.29 MeV) state in comparison to a collective model calculation (solid line), and a distorted-wave calculation using a charge transition density from inelastic electron scattering and a zero range force (dashed line). The dashed curve was normalized to match the magnitude of the data at the first maximum.

late these to neutron and proton multipole moments, the results imply that $M_n/M_p \approx 1$ for this nucleus.

ACKNOWLEDGMENTS

The authors would like to thank Dr. C. W. Glover, Dr. K. H. Hicks, Dr. G. R. Satchler, and Dr. R. L. Varner for useful comments. The Oak Ridge National Laboratory participants were supported by Martin Marietta Energy Systems, Inc. under Contract DE-AC05-84OR21400 with the U.S. Department of Energy. The University of Oregon and Oregon State University participants were supported in part by grants from the National Science Foundation.

*Also at Joint Institute for Heavy Ion Research, Oak Ridge, TN 37831. Present address: Indiana University Cyclotron Facility, 2401 Milo B. Sampson Lane, Bloomington, IN 47408.

[1]D. K. McDaniels, J. Lisantti, J. R. Tinsley, I. Bergqvist, L. W. Swenson, F. E. Bertrand, E. E. Gross, and D. J. Horen, Phys. Lett. **162B**, 277 (1985).

[2]K. W. Jones, C. Glashausser, R. de Swiniarski, S. Nanda, T. A. Carey, W. Cornelius, J. M. Moss, J. B. McClelland, J. R. Comfort, J.-L. Esudie, M. Gazzaly, N. Hintz, G. Igo, M. Jaji-Saeid, and C. A. Whitten, Jr., Phys. Rev. C **33**, 17 (1986).

[3]D. K. McDaniels, J. Lisantti, I. Bergqvist, L. W. Swenson, X. Y. Chen, D. J. Horen, F. E. Bertrand, E. E. Gross, C. Glover, R. Sayer, B. L. Burks, O. Häusser, and K. Hicks, Nucl. Phys. **A467**, 557 (1987).

[4]N. Marty, M. Morlet, A. Willis, V. Comparat, and R. Frascaria, Nucl. Phys. **A238**, 93 (1975).

[5]G. R. Satchler, Nucl. Phys. **A195**, 1 (1972); G. R. Satchler, *Direct Nuclear Reactions* (Oxford University Press, Oxford, 1983).

[6]F. E. Bertrand, E. E. Gross, D. J. Horen, J. R. Wu, J. Tinsley, D. K. McDaniels, L. W. Swenson, and R. Liljestrand, Phys. Lett. **103B**, 326 (1981).

[7]C. Djalali, N. Marty, M. Morlet, and A. Willis, Nucl. Phys. **A380**, 42 (1982).

[8]S. Kailas, P. P. Singh, D. L. Friesel, C. C. Foster, P. Schwandt, and J. Wiggins, Phys. Rev. C **29**, 2075 (1984).

[9]F. Osterfeld, J. Wambuch, H. Lenske, and J. Speth, Nucl. Phys. **A318**, 45 (1979).

[10]D. K. McDaniels, J. R. Tinsley, J. Lisantti, D. M. Drake, I. Bergqvist, L. W. Swenson, F. E. Bertrand, E. E. Gross, D. J. Horen, T. P. Sjoreen, R. Liljestrand, and H. Wilson, Phys. Rev. C **33**, 1943 (1986).

[11]F. E. Bertrand, E. E. Gross, D. J. Horen, J. Tinsley, D. K. McDaniels, J. Lisantti, L. W. Swenson, K. Jones, T. A. Corey, J. B. McClelland, and S. J. Seestrom-Morris, Phys. Rev. C **34**, 45 (1986).

[12]R. Finlay (private communication); T. S. Cheema and R. W. Finlay, Phys. Rev. C **37**, 910 (1988).

[13]N. M. Hintz, D. Cook, M. Gazzaly, M. A. Franey, M. L. Barlett, G. W. Hoffmann, R. Fergerson, J. McGill, J. B. McClelland, and K. W. Jones, Phys. Rev. C **37**, 692 (1988).

[14]D. Frekers, S. S. M. Wong, R. E. Azuma, T. E. Drake, J. D. King, L. Buchmann, R. Schubank, R. Abegg, K. P. Jackson, C. A. Miller, S. Yen, W. P. Alford, R. L. Helmer, C. Broude, S. Mattsson, and E. Rost, Phys. Rev. C **35**, 2236 (1987).

[15]H. S. Sherif, R. I. Sawafta, and E. D. Cooper, Nucl. Phys. **A449**, 709 (1986).

[16]K. K. Seth, D. Barlow, A. Saha, R. Soundranayagam, S. Iverson, M. Kaletka, M. Basko, D. Smith, G. W. Hoffmann, M. L. Barlett, R. Ferguson, J. McGill, and E. C. Milner, Phys. Lett. **158B**, 23 (1985).

[17]Jacques Raynal, Phys. Lett. B **196**, 7 (1987).

[18]D. A. Hutcheon (unpublished); (private communication).

[19]H. Sherif, Ph.D. dissertation, University of Washington, 1968; H. Sherif, Nucl. Phys. **A131**, 532 (1969).

[20]J. Raynal (unpublished); (private communication).

[21]R. I. T. Sawafta, M.S. thesis, University of Alberta, 1984.

[22]K. H. Hicks and J. Lisantti, Nucl. Phys. **A484**, 432 (1988).

[23]G. S. Adams, Th. S. Bauer, G. Igo, G. Pauletta, C. A. Whitten, Jr., A. Wriekat, G. W. Hoffmann, G. R. Smith, and M. Gazzaly, Phys. Rev. C **21**, 2485 (1980).

[24]A. M. Kobos, E. D. Cooper, J. I. Johansson, and H. S. Sherif, Nucl. Phys. **A445**, 605 (1985).

[25]A. M. Bernstein, V. R. Brown, and V. A. Madsen, Comments Nucl. Part. Phys. **2**, 203 (1983).

[26]M. M. Gazzaly, N. M. Hintz, G. S. Kyle, R. K. Owen, G. W. Hoffmann, M. Barlett, and G. Blanpled, Phys. Rev. C **25**, 408 (1982).

[27]M. L. Barlett, G. W. Hoffmann, and L. Ray, Phys. Rev. C **35**, 2185 (1987).

[28]A. Willis, B. Geoffrion, N. Marty, M. Morlet, C. Rolland, and B. Tatischeff, Nucl. Phys. **A112**, 417 (1968).

[29]J. Källne, G. Tibell, and A. Johansson, Phys. Scr. **2**, 195 (1970).

[30]W. J. Hornyak, J. C. Jacmart, M. Riov, J. P. Garron, Ch. Ruhla, and M. Liu, J. Phys. **24**, 1052 (1963).

[31]L. G. Arnold, B. C. Clark, R. L. Mercer, and P. Schwandt, Phys. Rev. C **23**, 1949 (1981).

[32]J. Lisantti, F. E. Bertrand, D. J. Horen, B. L. Burks, C. W. Glover, D. K. McDaniels, L. W. Swenson, X. Y. Chen, O. Häusser, and K. Hicks, Phys. Rev. C **37**, 2408 (1988).

[33]K. Itoh, M. Oyamada, and Y. Torizuka, Phys. Rev. C **2**, 2181 (1970).

[34]M. A. Franey and W. G. Love, Phys. Rev. C **31**, 488 (1985).